IEEE Access
Multidisciplinary | Rapid Review | Open Access Journal

Date of publication xxxx 00, 0000, date of current version xxxx 00, 0000.

Digital Object Identifier 10.1109/ACCESS.2024.0429000

Simplified Physical Stability Assessment of Chilean Mine Waste Storage Facilities Using GIS and AI: Application in the Antofagasta Region

GABRIEL HERMOSILLA[1], GABRIEL VILLAVICENCIO[2], GIOVANNI COCCA-GUARDIA[1] (Member, IEEE), VICENTE APRIGLIANO[2], MANUEL SILVA[1], (Member, IEEE), JUAN CARLOS QUEZADA[3], PIERRE BREUL[4], VINICIUS MINATOGAWA[2], JAIME MORALES[5]

[1]Escuela de Ingeniería Eléctrica, Pontificia Universidad Católica de Valparaíso, Valparaíso 2374631, Chile
[2]Escuela de Ingeniería de Construcción y Transporte, Pontificia Universidad Católica de Valparaíso, Valparaíso 2362804, Chile
[3]ICUBE, UMR 7357, CNRS, INSA de Strasbourg, Strasbourg, France
[4]Département Génie Civil, Polytech Clermont, Institut Pascal UMR CNRS 6602, Université Clermont Auvergne, Av. Blaise Pascal SA 60206-63178 Aubière, CEDEX, 63000 Clermont Ferrand, France
[5]Escuela de Ingeniería Química. Pontificia Universidad Católica de Valparaíso, Avenida Brasil 2180, Valparaíso 2362854, Chile

Corresponding author: Gabriel Hermosilla (e-mail: gabriel.hermosilla@pucv.cl).

This research was funded and supported by the Vice-Rectorate for Research, Creation, and Innovation (VINCI) at Pontificia Universidad Católica de Valparaíso (Chile), through the Associative Research Project DI (under grant: 039.301/2024), Centennial Project 2024 (under grant: 039.310/2024), and FONDECYT under Grant 1240573, and ANID Doctorado Nacional 2023-21232328.

ABSTRACT Chile's mining industry, a global leader in copper production, faces challenges due to increasing volumes of mining waste, particularly Waste Rock Dumps (WRD) and Leaching Waste Dumps (LWD). The National Service of Geology and Mining (SERNAGEOMIN) requires assessment of the physical stability (PS) of these facilities, but current methods are hindered by data scarcity and resource constraints. This study proposes a simplified evaluation methodology using first-order parameters from open-access data. By integrating Geographic Information Systems (GIS) and Artificial Intelligence (AI)—utilizing models like YOLOv11 and convolutional neural networks—we automate the detection and characterization of WRD and LWD from satellite imagery, extracting critical parameters for PS assessment. This approach reduces analysis time and minimizes human error. Validated in the Antofagasta Region, Chile's primary mining area, we identified and evaluated 70 WRD and 54 LWD. The results demonstrate the effectiveness of prioritizing deposits based on potential risk, enhancing SERNAGEOMIN's capacity for supervision. The successful application suggests scalability to other mining regions and adaptability to different facility types, including tailings storage facilities. This work offers a practical tool to improve safety and risk management in the mining industry, addressing critical challenges in PS evaluation under current regulatory constraints.

INDEX TERMS Artificial intelligence, closure plan, geographical information systems, mine waste storage facilities, physical stability assessment, Sentinel-2 satellite imagery, YOLOv11.

I. INTRODUCTION

THE mining industry in Chile, a world leader in copper production, generates a significant amount of mining waste, which is expected to progressively increase in the future. By 2026, Chile is projected to generate approximately 1,000 million tons of mining waste annually [1]. These materials are disposed of and stored in large structures known as Mine Waste Storage Facilities (MWSF).

Among these waste types are Waste Rock Dumps (WRD) and Leaching Waste Dumps (LWD), both of which are expected to increase in size and quantity in the near future. To date, more than 792 WRDs and LWDs zones have been identified [2], distributed across mining operations in regions I, II, III, IV, V, MR, VI, VII, and XI of Chile, reaching the following sizes: i) WRDs vary between 50 and 500 m in height, with projections up to 1,000 m in large mining projects, occupying thousands of hectares (Figure 1.a); ii) LWDs have heights ranging from 10 to 120 m and occupy areas covering hundreds of hectares (Figure 1.b).

To date, these types of MWSF have demonstrated adequate mechanical behavior under static and seismic conditions. However, in Chile, mining companies are legally obligated to assess and ensure their physical stability (PS), even after closure, to safeguard human life and health and to protect the

(a) (b)

FIGURE 1: MWSF under construction, located in the northern regions of Chile. a) Waste rock dumps (WRD), El Soldado, Nogales, Chile [3]. b) Leaching waste dumps (LWD), BioCobre, Copiapó, Chile [4].

environment, in accordance with national legislation [5], [6]. A potential failure in the PS of these facilities could result in to environmental disasters, significant material damage, and even loss of human life, as has been reported in other mining countries [7], [8].

The National Service of Geology and Mining (SERNAGEOMIN), a government entity responsible for the supervision and oversight of MWSF, faces a growing challenge due to the need to ensure the long-term PS of these mining facilities. To guide companies and inspectors in assessing PS, SERNAGEOMIN issued the "Methodological Guide for the Evaluation of the Physical Stability of Residual Mining Facilities" [9], hereinafter referred to as the PS Guide. This tool standardizes and regulates the procedures for evaluating the PS of MWSF. The evaluation process outlined int the PS Guide requires a range of physical parameters and environmental data, including both the design project and the closure plan for these facilities [5], [10]. Additionally, information from periodic monitoring conducted during their operation and construction phase is essential. Using this data, the PS Guide employs a matrix analysis to assess stability condition for various potential failure mechanisms. However, since its official adoption in 2018, the effective implementation of this evaluation and oversight tool has faced several technical barriers. These include the lack of a national MWSF registry, insufficient number of inspectors, difficulties in obtaining critical geotechnical parameters (e.g. foundation soils for MWSF), and stringent administrative requirements imposed by national regulations.

In this context, to address the current challenges associated with applying the PS Guide, this work proposes a simplified evaluation methodology. This methodology uses first-order parameters to estimate the global PS condition of WRD and LWD, using state-of-the-art technologies such as geographic information systems (GIS) and artificial intelligence (AI). GIS enables the integration and analysis of multiple layers of geospatial data, such as geology, topography, seismicity, and precipitation, complemented by specific geotechnical data on the waste [11], [12]. AI facilitates the automatic detection and geometric characterization of these deposits, reducing analysis times and minimizing human errors. This methodology, including proposed matrices and operational approach, will be validated through a case study in the Antofagasta Region, a key mining area in Chile with major operations (e.g., CODELCO and Antofagasta Minerals), to demonstrate its effectiveness. By integrating geospatial data layers and AI-based detectors, the methodology characterizes WRD and LWD and assesses critical stability parameters. This enables the development of a prioritization ranking for MWSF based on PS levels, facilitating effective supervision and oversight by SERNAGEOMIN. Furthermore, the methodology has potential applications in other mining regions and for different types of MWSF, such as tailings storage facilities (TSF).

II. RELATED WORK

The evaluation of the PS of MWSF has been a fundamental topic in research, due to the significant risks these facilities represent for human safety and the environment. Tradition-

ally, this evaluation relies on a series of factors and variables considered in geotechnical modeling to analyze possible failure modes (e.g., slope instability, static liquefaction, among others) during the design phase, as well as requiring periodic in-situ monitoring of each variable. However, economic resource constraints and the large scale of modern mining operations demand more efficient and scalable approaches. The following are some relevant studies in this field.

A. EVALUATION OF MWSF PS

In recent years, remote sensing techniques have transformed the evaluation of the PS of MWSF in engineering. For instance, satellites such as Sentinel-2 and Landsat have played a crucial role in providing high-resolution images and enabling continuous monitoring of the large areas occupied by MWSF. A recent study utilized the Google Earth Engine platform to process satellite images, optimizing information extraction from the deposits through image processing techniques and cloud cover reduction [13]. Another study demonstrated how machine learning algorithms can estimate parameters such as moisture content, facilitating operational periodic control in thickened tailings deposits [14].

In addition, remote monitoring technologies such as synthetic aperture radar (SAR) and interferometric radar (InSAR) have gained prominence in recent years for evaluating the PS of MWSF. These techniques enable the monitoring of surface deformation, which can serve as an early warning indicator for potential physical instability scenarios. Another example is the use of the Small Baseline Subset (SBAS) technique to monitor surface deformations in mining areas [15] [16]. These techniques have proven to be useful tools to complement classic geotechnical evaluations, offering continuous and real-time information.

B. ARTIFICIAL INTELLIGENCE IN THE DETECTION AND ANALYSIS OF MWSF

The integration of AI in the detection and analysis of MWSF has achieved remarkable progress in recent years, particularly for TSF. Object detection and segmentation models such as YOLO and Faster R-CNN have significantly improved the automatic identification of these mining facilities through satellite imagery [2], [17]. These models not only identify TSF with high precision but also enable the extraction of geometric and geotechnical parameters related to PS evaluation. Advances in deep learning have automated processes that previously required manual inspections, thereby increasing the efficiency of periodic monitoring.

Moreover, techniques for generating synthetic data have been developed to complement real datasets and improve the ability of AI models to learn and generalize across different scenarios. A recent example includes the use of generative adversarial networks (GANs) for creating synthetic data and parameters used in training regression models to estimate PS [18]. These innovations are facilitating a more automated and continuous analysis of TSF, a critical step toward improving risk management and mitigation for such mining facilities.

C. APPLICATIONS OF GIS IN MINING

The use of GIS has been fundamental for management and planning in the mining sector. GIS facilitates the integration and analysis of essential geospatial data, such as topography, geology, and hydrology, enabling informed decision-making regarding the location of new facilities and the environmental management of mining operations. In the context of PS evaluation, GIS provides a platform for overlaying multiple data layers, helping to identify critical spatial patterns influencing the PS of MWSF.

Several studies have implemented GIS methods to monitor, evaluate, or predict environmental or physical risks associated with TSF. For instance, [19], [20] applied GIS to identify historical and spatial patterns of incidents at such mining facilities and their relationship with climate variables, such as rainfall. In this regard, [20] used satellite images and GIS techniques to assess the risk level of TSF based on factors such as proximity to urban areas and the type of ore extracted. With an environmental focus, [21] applied a GIS-based method to assess the level of sediment storage and transport in rivers impacted by mining activity in Bolivia. [19] developed a GIS methodology to predict failures, using the Brumadinho case in Brazil as an example.

The combination of AI and GIS is proposed as an innovative strategy to improve the detection and evaluation of MWSF. GIS integrates multiple geographical data layers, while AI models analyze large volumes of satellite data, automating the identification of potential risks, obtaining critical parameters for PS evaluation, and optimizing resource management. This integrated approach prioritizes deposits with higher instability risks, offering a scalable solution to enhance safety in remote or hard-to-access areas.

III. PHYSICAL STABILITY OF WRD AND LWD

For the evaluation of the PS of WRD and LWD, SERNAGEOMIN as the supervisory body of the State of Chile, establishes that mining companies must use the classification system outlined in the PS Guide [9]. The objective is to facilitate progressive and safe closure processes for these types of MWSF. In general terms, the PS Guide was developed based on the framework of the systems initially proposed by [7] and later modified by [8] but including technical adaptations and criteria applicable to the context of the Chilean mining industry.

Currently, the PS Guide requires the evaluation of 20 factors or parameters that define PS, organized into 8 evaluation matrices (Table 1). To reflect the degree of importance on the PS of WRD and LWD, each factor is assigned a condition and a numerical rating, defined based on the analysis of the mechanical behavior observed in these types of MWSF [9]. The sum of these numerical ratings allows WRD and LWD to be evaluated and classified in terms of their PS level for the failure mechanisms being assessed: slope instability/foundation instability and static liquefaction. A higher numerical rating corresponds to a lower PS level and a greater associated failure occurrence potential (FOP) (Figure 2). It is important

TABLE 1: Evaluation Matrix for PS Assessment

ID	Matrix	Factor or attribute
M1	Foundation conditions	Geomechanical characteristics of foundation soil, shape foundation, and MWSF typology.
M2	Geometric configuration	Overall height, overall fill slope angle, maximum thickness lift, and maximum overall thickness.
M3	Constructive background	Construction method and loading rate.
M4	Material quality and in-situ state	Particle size distribution, Atterberg limits, and in-situ state condition.
M5	Instrumentation and monitoring	Piezometrics levels, drainage systems, accelerometers, and inclinometers.
M6	Regional setting for the closure condition	Seismicity and precipitation (rain and/or snow).
M7	Stability performance	PS observed during the operational phase.
M8	Degree of implementation of measures to ensure PS in the operation and closure stages	Verification of works and actions implemented as indicated in the approved closure plan.

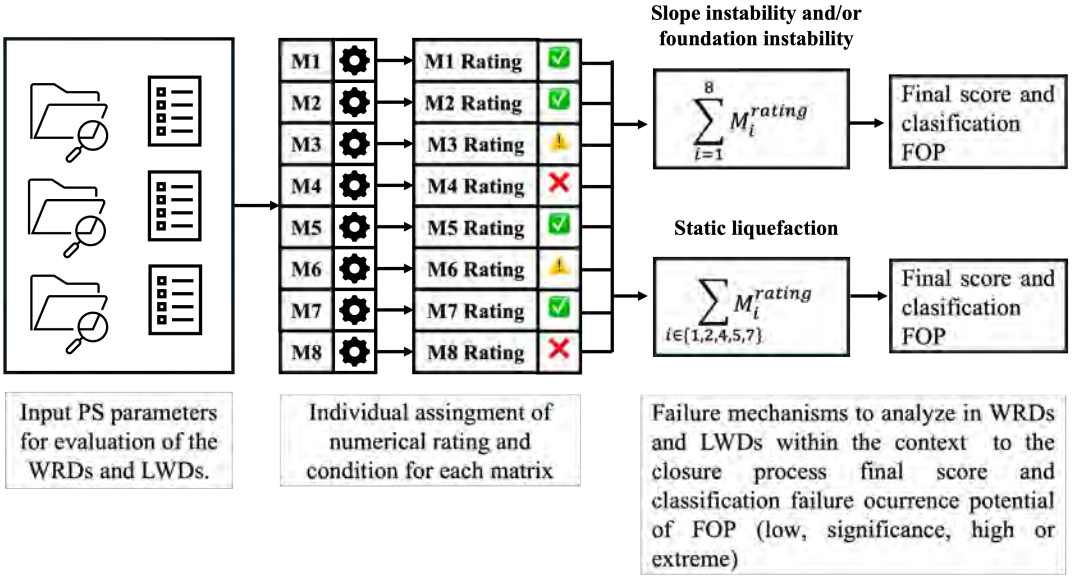

FIGURE 2: Evaluation scheme of WRD and LWD according to the PS Guide [9].

to note that this evaluation system was defined by a committee of national and international experts and subsequently applied in various national mining operations for calibration.

Although this classification system uses various parameters from technical reports that mining companies are required to submit to SERNAGEOMIN (such as the design project and closure plan), and basic operational control of these MWSF (geometric configuration, construction background, instrumentation and monitoring, stability performance, among others), it has been evidenced that this information is limited or, in many cases, inaccessible due to poor management and lack of updates of the required information. This has hindered the effective application of the PS Guide for both mining companies and SERNAGEOMIN.

This context has affected SERNAGEOMIN's supervisory role, particularly in the case of WRD and LWD, facing various obstacles: i) the absence of a national registry for these types of MWSF; ii) a shortage of inspectors nationalwide; iii) the large number of variables required to evaluate PS, many of which lack quantifiable information; iv) technical and economic difficulties in obtaining critical parameters, such as soil conditions, geometric configuration, and geotechnical characteristics; v) strict administrative requirements imposed by current national regulations. These challenges highlight the need for a more efficient and updated system that enhaces both supervision and compliance with safety standards in the management of MWSF.

Given the limitations of the PS Guide for evaluating the PS of WRD and LWD, we propose a simplified system to overcome data scarcity by using open-source information. This proposal relies on geospatial data such as surface geology, active faults, seismicity, topography, and precipitation. In addition, it considers general knowledge of the geomechanical properties of WRD and LWD [11], [12] , complemented by advanced GIS and AI technologies for automated data processing, while generally maintaining the evaluation criteria defined in the PS Guide [9].

IV. PROPOSED PS EVALUATION USING SIMPLIFIED MATRICES

The proposed simplified system, developed with the participation of expert engineers from SERNAGEOMIN, reorganizes the eight original matrices from the PS Guide into four key matrices. These matrices focus on foundation conditions, geometric configuration, geomechanical quality of the material, and the regional setting of the deposits (Figure 3). The excluded matrices (M3: constructive background; M5: instrumentation and monitoring; M7: stability performance; and M8: degree of implementation of measures to ensure PS in the operation and closure stages) rely on data that, to date, are not regularly recorded or monitored during the construction and operation phases of these types of mining facilities. Thus, simplifying and adapting the PS Guide is essential to enable more frequent and accessible evaluations, especially for MWSF that lack records and are not regularly monitored.

Each matrix uses open-access data, enabling scalable and practical implementation. The sum of the scores from each matrix results in the Physical Global Stability Index (PSGI), a qualitative measure that facilitates the prioritization of deposits for SERNAGEOMIN supervision, focusing on those with the highest potential risk. The simplified matrices are presented below.

A. MATRIX M1′: FOUNDATION CONDITIONS

Foundation conditions include key factors for the PS of WRD and LWD, especially for instabilities associated with foundation failures, such as rotational failure, non-circular rotation, wedge failure, base translation, liquefaction, and toe failure [7]–[9]. In this context, the parameters included in this matrix are related to the characteristics of the foundation soil: overburden type and topography.

The foundation soil types of WRD and LWD, in a first approximation, can be defined based on their geological origin (rock and residual or sedimentary soils). A complementary parameter, widely used to define seismic site characterization, is the stiffness upper 30 m of the soil profile through an equivalent shear wave velocity Vs_{30} [22]. The foundation soil topography has been linked to the average overall foundation slope angle (α) and the foundation shape of the area where the WRD and LWD are located, as shown in Figure 4.2a and Figure 4.2b, respectively. The parameter α corresponds to the angle between the toe of the WRD and LWD slopes and their upper intersection with the natural terrain.

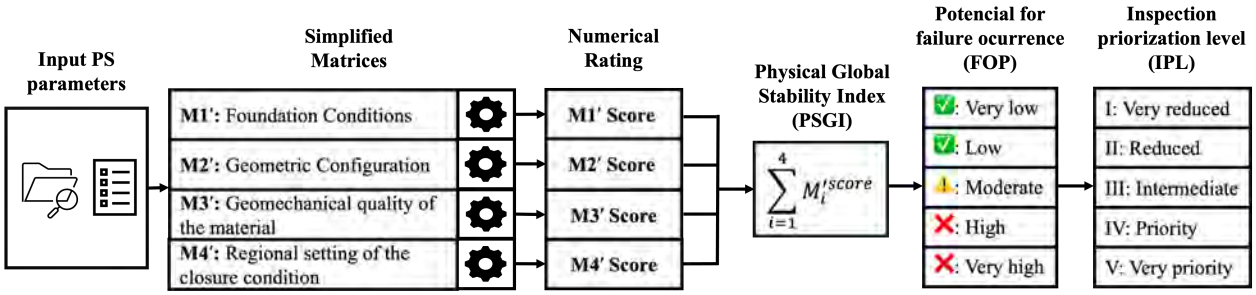

FIGURE 3: Simplified evaluation system of global PS and inspection prioritization of WRD and LWD.

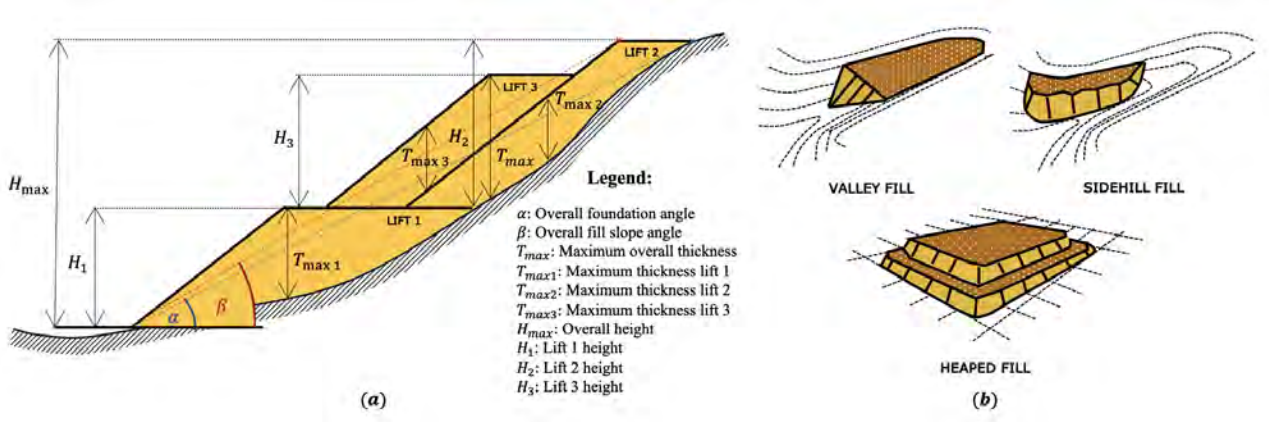

FIGURE 4: Geometric parameters and typology of WRDs and LWDs. a) Geometric parameters of WRDs and LWDs. b) Basic MWFs types. Adapted from [8].

TABLE 2: Evaluation matrix M1': foundation conditions factors

Factor	Parameter and condition	Category	Ratings
Geomechanical characteristics of foundation soil	Type I: rock and $Vs_{30} > 900$ (m/s)	Very competent	0
	Type II: soft or fractured rock, very dense or hard soils and $Vs_{30} \geq 500$ (m/s)	Competent	100
	Type III: dense or very stiff soils and $Vs_{30} \geq 350$ (m/s)	Intermediate	200
	Type III: medium-dense or firm to stiff soils and $Vs_{30} \geq 180$ (m/s)	Weak	300
	Type IV: loose to medium-dense or soft to firm soils and $Vs_{30} < 180$ (m/s)	Very weak	400
Average overall foundation slope angle (α)	5°	Flat	0
	5 – 15°	Gentle	50
	15 – 25°	Moderate	100
	25 – 32°	Steep	150
	> 32°	Very steep	200
	No information	–	200
Shape foundation/MWSF typology	Valley fill or cross valley fill	Confined	0
	Sidehill fill	Moderately confined	100
	Heaped fill or ridge crest fill	Unconfined	200
	No information	–	200

TABLE 3: Evaluation matrix M2': geometric configuration factors

Factor	Parameter and condition		Ratings
Overall height (m)	< 100		0
	100 – 250		50
	250 – 500		100
	> 500		200
	No information		200
Volume (m^3)	Small	< 10,000,000	0
	Medium	10,000,000 – 100,000,000	50
	Large	100,000,000 – 1,000,000,000	100
	Very large	> 1,000,000,000	200
	No information		200
Overall fill slope angle (β°)	Gentle	< 26	0
	Moderate	26 – 34	50
	Steep	34 – 39	100
	Very steep	> 39	200
	No information		200
Lifts	With lifts		0
	Without lifts		200
	No information		200

The structure of matrix M1' is presented in Table 2. To obtain the evaluation parameters contained in matrix M1', the following open-source layers were used: i) Geomechanical characteristics of foundation soil: geological map of Chile, scale 1:1,000,000 [23] and Vs_{30}: Global Vs_{30} mosaic map viewer [24]; ii) foundation soil slope and shape foundation/MWSF typology: ground slope (slope geoprocessing of digital elevation models [25], and open-access satellite images (Sentinel-2).

B. MATRIX M2': GEOMETRIC CONFIGURATION

The geometric configuration of WRD and LWD defines the PSGI level they present, associated with the generation of the following failure mechanisms: edge slumping, plane failure, and rotational failure [7]–[9]. The geometric parameters (Figure 4) are directly related to the shape and size of these types of MWSF. For simplified evaluation purposes, the proposed matrix M2' includes the following geometric parameters: overall height, volume, overall fill slope angle, and stepped construction (single or multiples lifts), as presented in Table 3 These geometric parameters are obtained from the processing and analysis of satellite images (Sentinel-2). For the single lift slope angle, based on topographic surveys from WRD and LWD design projects, [12] propose a range of 34-39º for WRD. Meanwhile, [11] suggest a range of 33-35º for LWD.

TABLE 4: Evaluation matrix M3': geomechanical quality factors of waste rock and leached ore material

Parameter and condition	Category	Ratings
Very coarse grained (WRD): - % fines (passing # 200 sieve; < 0.075 mm) < 10% - % great than 3" > 50% - Plasticity: N/A - Intact strength: very strong to strong (UCS > 100 MPa) - Durability: very high to high	High	0
Mixed grained (LWD): - % fines (passing # 200 sieve; < 0.075 mm), between 10-25% - % great than 3", between 25-50% - Low plasticity: LL < 35%; PI < 10% - Intact strength: medium strong (UCS: 50 - 100 MPa) - Durability: medium high	Moderate	100
No information	–	200

TABLE 5: Evaluation matrix M4': regional setting for the closure condition of WRD and LWD

Parameter	Description	Condition	Category	Ratings
Seismicity	Peak Ground Acceleration (PGA) or A_0, based on seismic zones of Chile (INN, 2012)	$A_0 \leq 0.2g$	Low	0
		A_0: 0.2g – 0.3g	Moderate	200
		$A_0 > 0.4g$	High	400
Distance to active and potentially-active continental faults	Distance from the trace of faults (polygon defined at 300m distance from the fault trace)	Outside the polygon	Low	0
		Inside the polygon	High	200
Precipitation	Average annual rainfall and/or snowfall	Rainfall < 100 (mm) Snowfall < 10 (cm)	Very low	0
		Rainfall: 100 – 350 (mm) Snowfall: 10 – 35 (cm)	Low	100
		Rainfall: 350 – 1000 (mm) Snowfall: 35 – 100 (cm)	Moderate	200
		Rainfall: 1000 – 2000 (mm) Snowfall: 100 – 200 (cm)	High	300
		Rainfall > 2000 (mm) Snowfall > 200 (cm)	Very high	400

TABLE 6: ILP in WRD and LWD, based on PSGI and FOP

PSGI	FOP	IPL
< 600	Very low	I: very reduced
[600 – 1200[	Low	II: reduced
[1200 – 1800[	Moderate	III: moderate
[1800 – 2200[	High	IV: priority
[2200 – 2800]	Very high	V: very priority

C. MATRIX M3': GEOMECHANICAL QUALITY OF THE MATERIAL

The geomechanical properties of WRD and LWD, such as gradation (particle size distribution, PSD), plasticity of fines (Plasticity Index, PI, and Liquid Limit, LL), intact strength (Uniaxial Compressive Strength, UCS), and durability (Slake Durability Index, SDI), among others, are considered key factors influencing overall PS [7], [8]. Although these MWSF are not usually characterized during the construction and operation phases through in-situ and laboratory tests, recently [11], [12] proposed databases with variation ranges for PSD, plasticity, intact strength, and durability of waste rock and leached ore materials generated by the copper mining industry in Chile. Based on this information, it is possible to globally define the geomechanical quality depending on the type of identified MWSF, which will be used to apply matrix M3' (Table 4).

D. MATRIX M4': REGIONAL SETTING FOR THE CLOSURE CONDITION

To consider the regional setting where WRD and LWD are located, in the national context for the closure condition of these MWSF, the following parameters have been considered: seismicity, precipitation (rain and/or snow), and active and potentially active continental faults, which form matrix M4' (Table 5). The open-source data layers used for matrix M4' are as follows: i) seismicity: seismic zones of Chile [26] created in the context of this work using open-source GIS; ii) geological faults: database of active and potentially active continental faults in Chile at a 1:25,000 scale [27]; iii) precipitation: layers from the National Information System of Groundwater of Chile [28].

E. CALCULATION OF THE PSGI

The PSGI is calculated by summing the scores obtained in each matrix (Eq. 1). The PSGI provides a qualitative approximation of the PS global of the MWSF, linked to FOP and with an inspection prioritization level (IPL) (Table 6). This classification enables the prioritization of inspector actions and resource allocation by SERNAGEOMIN, focusing on WRD and LWD that present the highest PSGI.

$$\text{PSGI} = \sum_{\text{rating}} M1' + \sum_{\text{rating}} M2' + \sum_{\text{rating}} M3' + \sum_{\text{rating}} M4' \quad (1)$$

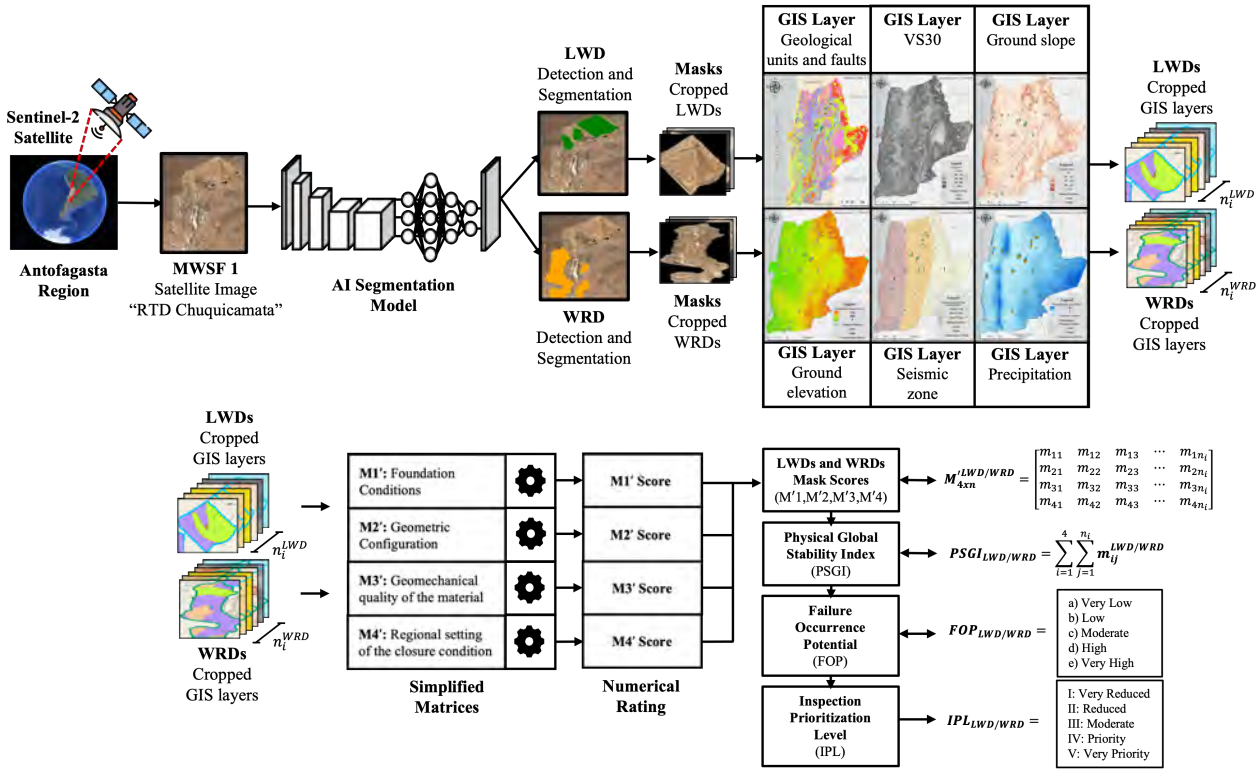

FIGURE 5: Overview of the Proposed Methodology automate the PS evaluation of the global PS for WRD and LWD.

V. METHODOLOGY

To automate the PS evaluation process using the proposed simplified matrices, remote sensing, GIS, and artificial intelligence techniques will be used. This methodology is organized into several key stages, including:

- Creation of the WRD and LWD database.
- Automatic detection and segmentation of WRD and LWD deposits.
- Integration of GIS layers.
- Application of AI models to the proposed matrices.
- Automatic evaluation of the global PS through simplified matrices.
- Calculation of the PSGI and categorization of WRD and LWD deposits.

Figure 5 illustrates the overall flow of the proposed methodology, applied to the Antofagasta region in Chile, which represents both state-owned and private companies involved in large- and medium-scale mining. The flow shows how PS is evaluated through the detection and segmentation of WRD and LWD using satellite images processed by an AI model. The detected deposits are georeferenced within GIS layers to obtain the parameters needed for evaluation in the simplified matrices, followed by categorization and prioritization.

A. DATABASE: WRD AND LWD

To date, SERNAGEOMIN does not have an official registry of WRD and LWD. The Atlas de Faenas Mineras, an official SERNAGEOMIN database with information on mining operations approved until 2020, was used to define the search area for WRD and LWD, potentially including nearby MWSF.

Using this approach, images of the mining areas available in the Atlas for the Antofagasta Region were downloaded using the Sentinel-2 satellite API, considering 16 instances between 2023 and 2024 for each mining area at the maximum available resolution of 10x10 m/px. Labeling of WRD and LWD was conducted using Label-Studio software [29], with input from a geotechnical expert.

The images were stored in the following filename format to maintain the geolocation of the area: "[x_min,y_min,x_max,y_max] - (date) - band.png", where (x,y) corresponds to (longitude, latitude), "(date)" refers to the date of the mining area, and "band" is the name of the band downloaded from Sentinel-2, which in this case corresponds to RGB. A total of 2,500 images were downloaded, of which 1,733 were labeled after discarding those with clouds or noise. The labeled dataset was divided into a training set (75%) and a test set (25%), ensuring that the first 12 instances of each mining area were used for training, while the last 4 instances were reserved for testing. The details of the downloaded and labeled database are provided in Table 7.

B. AUTOMATIC DETECTION AND SEGMENTATION OF WRD AND LWD

For detecting and segmenting WRD and LWD, the YOLOv11 model was chosen for its efficiency and accuracy in satellite

TABLE 7: Distribution of the database used for training the YOLOv11 segmentation model

	Total (100%)	Train (75%)	Test (25%)
Images	1,733	1,268	465
WRD	5,206	3,853	1,353
LWD	2,532	1,873	659

TABLE 8: Evaluation metrics results of the trained YOLOv11 segmentation model

Class	Metric	Precision	Recall	mAP50	mAP50-95
All	bbox	0.998	0.608	0.804	0.773
	segm	0.995	0.606	0.802	0.680
WRD	bbox	**0.999**	0.614	0.807	0.776
	segm	0.993	0.610	0.803	0.665
LWD	bbox	0.996	**0.716**	**0.857**	**0.832**
	segm	0.992	0.713	0.855	0.762

image analysis [30] [2]. YOLOv11 was selected due to its superior performance in processing high-resolution satellite images, its capability to handle complex object shapes, and its balance between speed and precision, making it well-suited for large-scale mining applications. Fine-tuning was performed using the "YOLOv11x-seg" weights on the labeled database, which allowed the detections to be specifically adapted to the deposits of interest. This fine-tuning was validated using the test set, employing metrics such as precision, recall, and mAP to evaluate model performance.

The results of these metrics, presented in Table 8, indicate that the YOLOv11 model successfully detected all labeled deposits, achieving a precision of up to 0.998 for bounding box detection and 0.995 for segmentation. Despite this high precision, slightly lower recall values indicate some additional false positives, which may be attributed to the presence of visually similar features in the satellite images. These false positives may affect the overall evaluation process by increasing the need for additional verification steps to ensure accuracy. Notably, the model performed exceptionally well in detecting LWD, with mAP50 values of 0.857 for bounding boxes and 0.855 for segmentation. The high precision of YOLOv11 in detecting WRD and LWD ensures high confidence in the automatic evaluation process of global PS. This precision enables the effective integration of segmented masks with GIS elevation and slope layers for a comprehensive analysis of the geospatial characteristics of the WRD and LWD.

C. INTEGRATION OF GIS LAYERS

Once the YOLOv11 model was trained, it was used to detect and segment WRD and LWD in mining areas of interest, which were then processed alongside GIS layers. The GIS layers used in the matrix evaluation are described in Annex A. These layers have a resolution of 12.5x12.5 m/px, which differs from the satellite image resolution of 10x10 m/px used in the database. This difference in resolution occurs because GIS layers are typically optimized for regional-scale analysis, whereas satellite images are captured at a finer resolution to provide detailed local information. The detections made by YOLOv11 are adjusted to match the GIS layer size before processing the segmented deposits, which might slightly impact the accuracy of parameter extraction due to scaling adjustments.

Thus, the bounding boxes obtained from YOLOv11 detection are used to crop WRD and LWD deposits, preserving their aspect ratio relative to the original image. Preserving the aspect ratio helps maintain the accuracy of georeferencing by avoiding distortions during parameter extraction. The masks resulting from the segmentations performed by YOLOv11 are used to georeference the deposits within the GIS layers to obtain the parameters needed for PS evaluation through the proposed simplified matrices.

D. APPLICATION OF AI MODELS TO THE PROPOSED MATRICES

To evaluate the proposed matrices, most parameters are obtained from GIS layers. However, matrices M1' and M2' require visual and geometric parameters, such shape foundation/MWSF typology (degree of confinement) and the presence of lifts in WRD and LWD. For these cases, two multiclass classification models were trained: one to determine shape foundation/MWSF typology (degree of confinement) and another to identify the presence or absence of lifts (as shown in Figure 4b).

A ResNet18 neural network [31], a variant of the residual network architecture, was used for these classifiers. ResNet18 was chosen due to its ability to mitigate the vanishing gradient problem, its efficiency in training on relatively smaller datasets, and its proven effectiveness in learning complex patterns, making it well-suited for this specific classification task. A new database was generated from the segmented masks of the initial database, manually labeled with an expert's assistance, to train these models. A balanced set of classes was obtained and divided into training (80%), validation (10%), and test (10%) sets, totaling 5,940 labeled deposits for the presence of lifts and 10,800 MWSF with degree of confinement levels. The class distribution is detailed in Table 9.

The evaluation metrics for the degree of confinement classifier showed outstanding results, with precision ranging from 0.92 to 0.99 and an F1-score from 0.96 to 0.99 across all classes (see Table 10). These metrics indicate the model's high reliability in accurately classifying the degree of confinement, which is crucial for understanding the structural stability of the deposits. For the lift classifier, results also showed high precision and recall, reaching values between 0.96 and 1.00 across all classes and datasets. These results, detailed in Table 11, demonstrate excellent classification capabilities for distinguishing between MWSF with and without lifts.

TABLE 9: Details of the database used to train the lifts classification model and confinement classification model

Multiclass classifier model	Category	Total (100%)	Train (80%)	Val (10%)	Test (10%)
Lifts classifier	With lifts	2,970	2,376	297	297
	Without lifts	2,970	2,376	297	297
Confinement classifier	Valley fill	2,700	1,889	405	406
	Sidehill fill	2,700	1,889	405	406
	Heaped fill	2,700	1,889	405	406

TABLE 10: Evaluation metrics results of the trained confinement classifier model

Metric	Valley fill	Sidehill fill	Heaped fill
Precision	0.920	0.953	0.985
Recall	0.931	0.919	0.990
F1-score	0.967	0.945	0.980

TABLE 11: Evaluation metrics results of the trained lifts classifier model

Metric	With lift	Without lift
Precision	1.000	0.997
Recall	0.997	1.000
F1-score	0.998	0.998

E. AUTOMATIC EVALUATION OF GLOBAL PS THROUGH SIMPLIFIED MATRICES

The automatic evaluation of the global PS of WRD and LWD integrates detection, segmentation, and geospatial analysis, supported by the trained YOLOv11 model (Table 12). The resulting masks are georeferenced within GIS layers to extract parameters for each evaluation matrix. Trained multiclass classifiers are essential for extracting geometric parameters, such as the presence of lifts or the degree of confinement. This automated approach relies on consistent data quality, which may limit accuracy in areas with incomplete or outdated information. Once a WRD or LWD is evaluated, the PSGI is calculated using the following expression:

$$\text{PSGI} = \sum_{i=1}^{4} \sum_{j=1}^{n_i} m_{ij}^{\text{score}} \tag{2}$$

Where m_{ij}^{score} the score obtained after evaluating factor j within matrix i, and n_i represents the total number of factors corresponding to matrix i for each WRD or LWD detected.

VI. EXPERIMENTS AND RESULTS

Two experiments were conducted to validate the proposed methodology for evaluating the PS WRD and LWD. The first experiment applied the methodology to a case study at the Radomiro Tomic Division (RTD), Chuquicamata South Mine (Antofagasta region, Chile), involving satellite imagery acquisition using Sentinel-2, segmentation with YOLOv11, and parameter extraction through GIS georeferencing. Multiclass classification models assessed structural features like the degree of confinement and presence of lifts. The second experiment applied the methodology to all available images from the Antofagasta region to generate a comprehensive PS assessment of WRD and LWD, with the aim of creating a proposed official registry to assist in the inspection and supervision by SERNAGEOMIN.

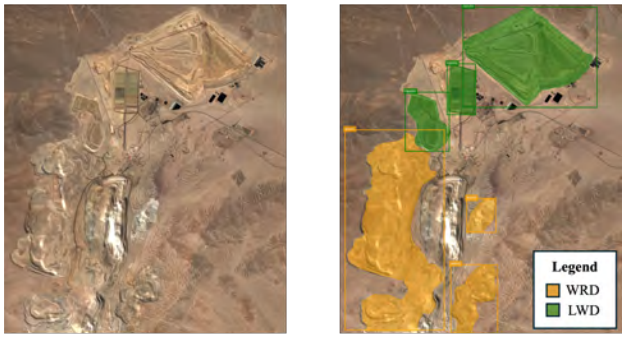

(a) (b)

FIGURE 6: Detection and segmentation results of the case study. (a) Unprocessed mining area. (b) Mining area segmented into WRDs and LWDs by YOLOv11.

A. EXPERIMENT 1: AUTOMATIC EVALUATION OF PS AT THE RTD

Figure 6 shows a satellite image of the mining area under study, along with the corresponding detection and segmentation performed by YOLOv11. The model demonstrated effective detection and segmentation of MWSF in the mining area, accurately delineating the WRD and LWD boundaries and minimizing false positives. For RTD Chuquicamata South Mine, 3 WRD zones and 3 LWD zones were detected, covering a total area of 1327.03 (ha) and 986.53 (ha), respectively.

Following detection, the segmented masks were georeferenced within GIS layers, including geological units, active and potentially active continental faults, Vs_{30} parameter, ground slope, seismic zone, and precipitation layers, to extract specific parameters needed for evaluating each of the proposed matrices (Figures A.3 and A.2). By integrating these GIS data, a detailed PS assessment of the detected WRD and LWD was performed using simplified evaluation matrices, ensuring that each aspect of the physical environment was accurately considered.

Subsequently, multiclass classification models were used to determine the degree of confinement (shape foundation/MWSF typology) and the presence of lifts in each de-

TABLE 12: Materials required for automatic evaluation of the global PS for WRD and LWD

Matrix	Factors	Materials	Scores
M'1	Geomechanical characteristics of foundation soil	Mask + GIS Geology layer + GIS V_{S30} layer	m_{11}^{score}
	Average overall foundation slope angle (α)	Mask + GIS ground slope layer	m_{12}^{score}
	Shape foundation and MWSF typology	Mask + Confinement classifier	m_{13}^{score}
M'2	Overall height	Mask + GIS ground elevation layer	m_{21}^{score}
	Volume	Mask + GIS ground elevation layer	m_{22}^{score}
	Overall fill slope angle (β)	Mask + Lift classifier	m_{23}^{score}
	Lifts	Mask + Lift classifier	m_{24}^{score}
M'3	Geomechanical quality	Mask and material database	m_{31}^{score}
M'4	Seismicity	Mask + GIS seismic zones layer	m_{41}^{score}
	Distance to geological faults	Mask + GIS active and potentially-active continental faults	m_{42}^{score}
	Precipitation	Mask + GIS precipitation layer	m_{43}^{score}

TABLE 13: Results of the evaluation of global PS for each detected WRDs and LWDs in the case study mining area

Rating	Mask ID 1	Mask ID 2	Mask ID 3	Mask ID 4	Mask ID 5	Mask ID 6
m_{11}^{score}	200	100	100	300	300	300
m_{12}^{score}	50	0	100	50	0	50
m_{13}^{score}	200	200	200	200	200	200
m_{21}^{score}	200	200	200	200	200	200
m_{22}^{score}	200	200	200	200	200	200
m_{23}^{score}	50	0	0	0	0	0
m_{24}^{score}	0	200	200	200	200	200
m_{31}^{score}	200	200	0	0	200	0
m_{41}^{score}	200	200	200	200	0	0
m_{42}^{score}	200	200	200	200	0	0
m_{43}^{score}	0	0	0	0	0	0
PSGI	1300	1300	1200	1350	1300	1150
FOP	Moderate	Moderate	Moderate	Moderate	Moderate	Low
IPL	III	III	III	III	III	II

tected WRD and LWD in the studied mining area. The results are presented in Figure 9. This workflow ensured a consistent evaluation of each WRD and LWD using the proposed matrices, with a summary of the scores obtained for each matrix shown in Table 13. Detailed ratings for each evaluation matrix, along with the resulting PSGI score, FOP, and associated IPL, are also included.

B. EXPERIMENT 2: APPLICATION OF THE METHODOLOGY IN THE ANTOFAGASTA REGION, CHILE

In the second experiment, the methodology was expanded to cover the entire Antofagasta region, using all available satellite images to conduct a comprehensive assessment of existing WRDs and LWDs. By processing these images, an Excel file was generated containing detailed information on each mining area, including central geolocation and detected WRD and LWD. This Excel file serves as a valuable tool for stakeholders, such as SERNAGEOMIN, to improve monitoring and management efforts by providing centralized, accessible data on deposit locations and characteristics. As SERNAGEOMIN currently lacks an updated registry, our work provides a critical foundation for their oversight efforts.

The generated Excel file also formed the basis for projecting the detected WRD and LWD on a map of the Antofagasta region, offering a clear visual representation of the deposits and their corresponding locations (Figure 10a). Table 14 provides details on the number of detected mining facilities and MWSF, including 70 WRD and 54 LWD deposits, along with their categorization based on FOP and IPL (Figure 10b). This categorization is crucial for prioritizing inspections or interventions, allowing SERNAGEOMIN to allocate resources efficiently and focus on areas of higher risk. By providing an updated registry, our work supports SERNAGEOMIN's efforts to improve their regulatory oversight and management capabilities across the region.

TABLE 14: Results of the evaluation of global PS of WRDs and LWDs in the Antofagasta region

FOP	IPL	MWFS	WRD	LWD
Very low	I: Very reduced	0	0	0
Low	II: Reduced	18	13	5
Moderate	III: Moderate	105	57	48
High	IV: Priority	1	0	1
Very high	V: Very priority	0	0	0

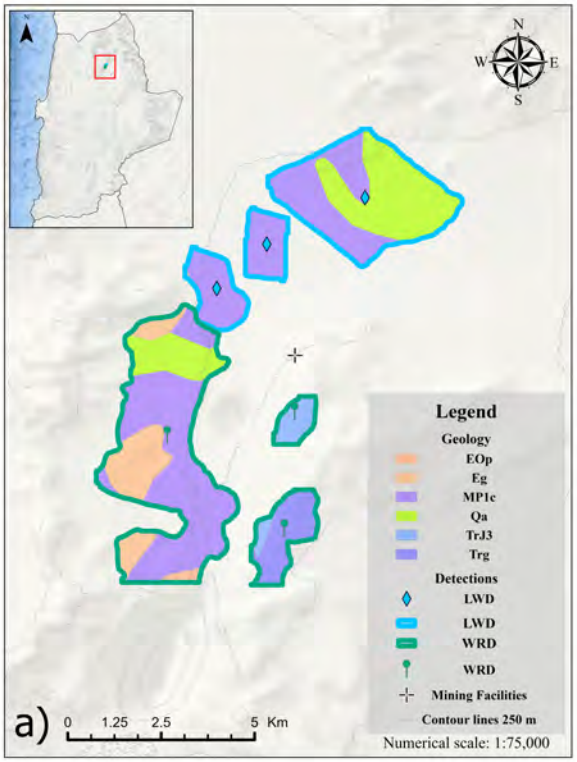

(a) Geological units.

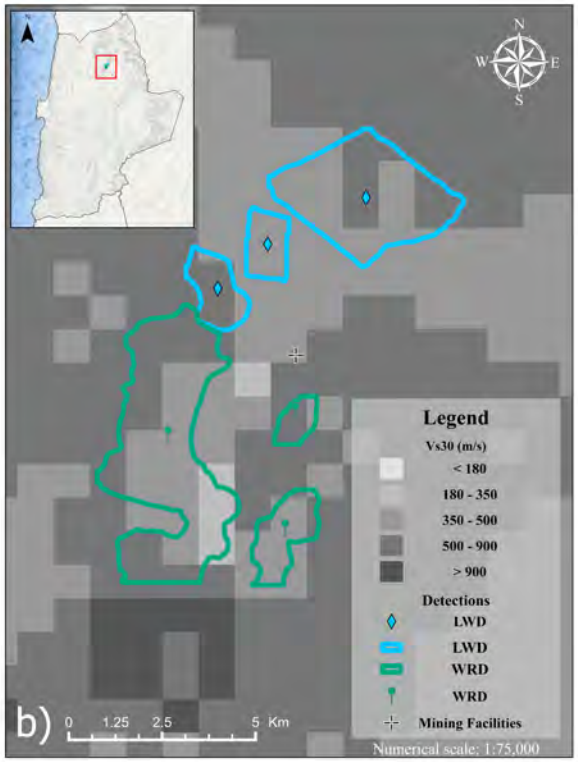

(b) Global Vs_{30} values.

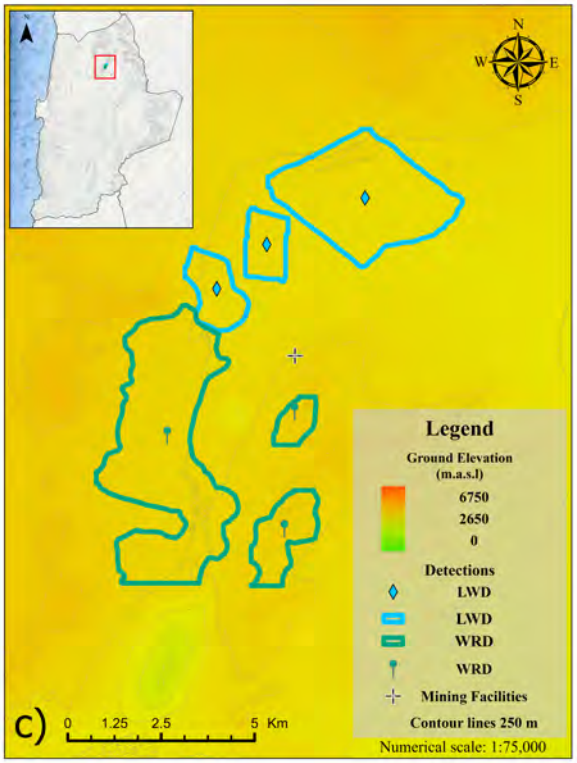

(c) Ground elevation.

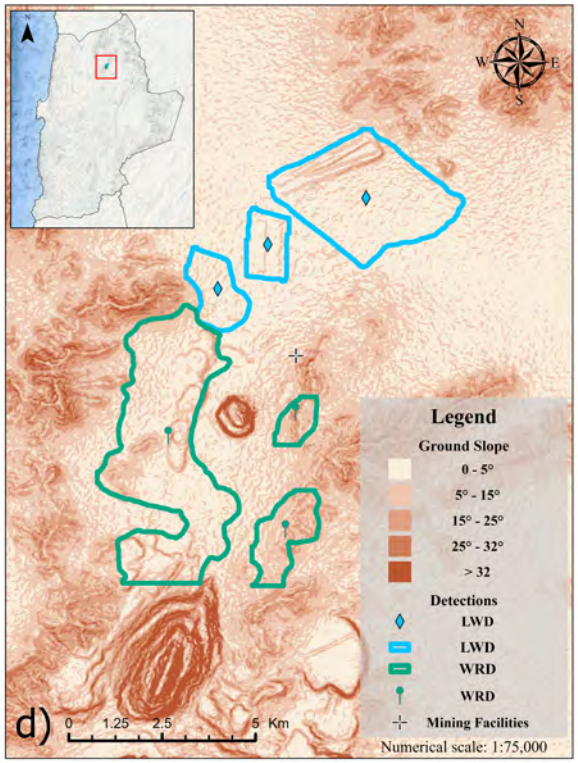

(d) Ground slope.

FIGURE 7: Detection and segmentation of WRDs and LWDs in Chuquicamata, South Mine (CODELCO), georeferenced within GIS layers.

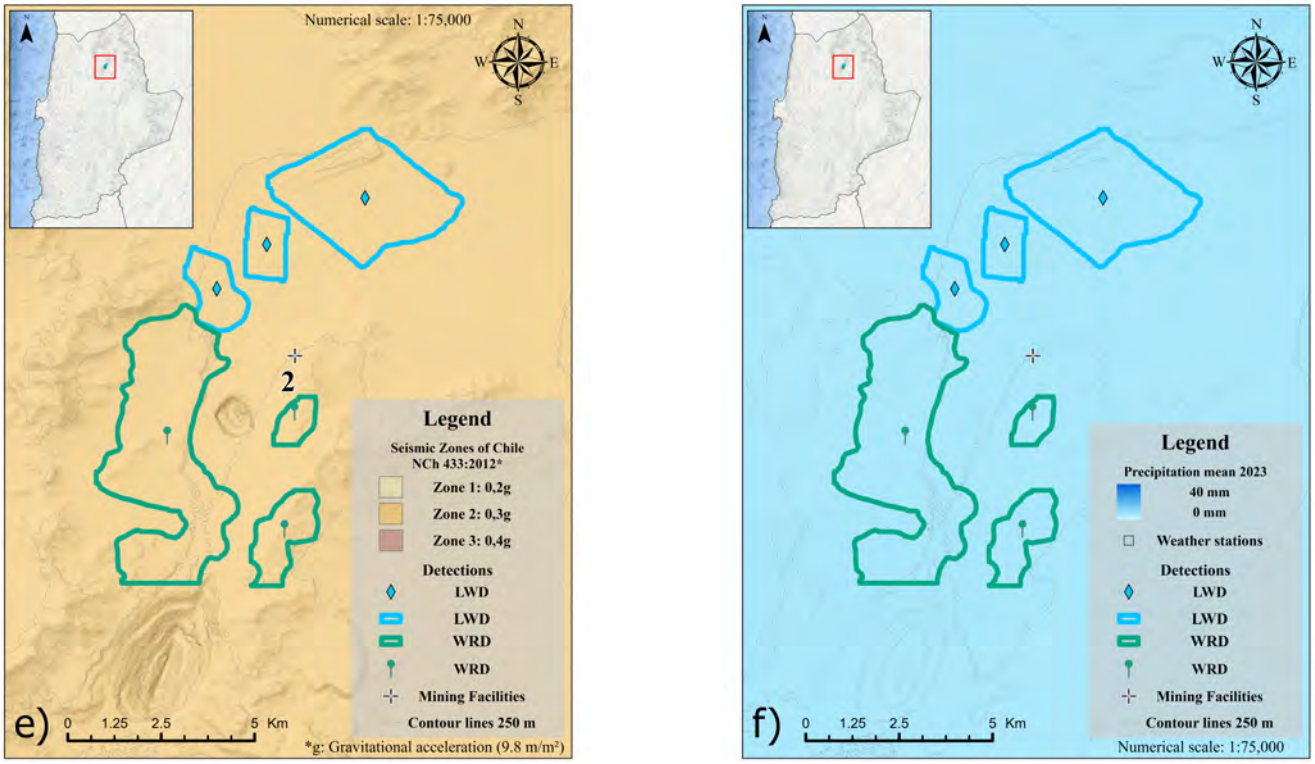

FIGURE 8: Detection and segmentation of WRDs and LWDs in Chuquicamata, South Mine (CODELCO), georeferenced within GIS layers: a) Seismic zone. b) Precipitations.

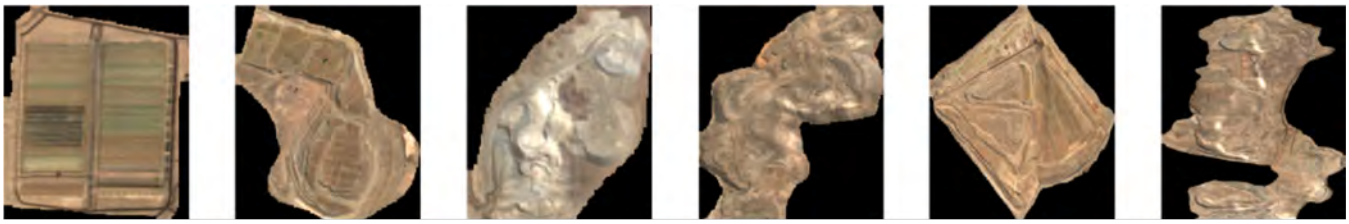

FIGURE 9: Detection, lift classifier and confinement classifier results shown as: Class, lift presence and typology. (a) LWD, Without lift, Heaped fill. (b) LWD, With lift, Heaped fill. (c) WRD, With lift, Heaped fill. (d) WRD, With lift, Heaped fill. (e) LWD, With lift, Heaped fill. (f) WRD, With lift, Heaped fill

VII. CONCLUSION

The present work introduces an innovative solution to the challenges in evaluating the physical stability of WRD and LWD in Chile. The proposal of simplified matrices represents a significant advancement, enabling SERNAGEOMIN to overcome current data and resource limitations. By focusing on first-order parameters obtainable through open-access information, these matrices simplify and streamline the evaluation process without compromising accuracy.

The integration of GIS technologies and AI techniques has proven highly effective in the automatic detection and characterization of WRD and LWD. The developed methodology utilizes detection and classification models, such as YOLOv11 and convolutional neural networks, to analyze satellite images and extract critical parameters for PS evaluation. This approach not only reduces analysis times and minimizes human errors but also allows for significant scalability and adaptability.

The validation of the methodology in the Antofagasta Region, a key mining area in Chile, enabled the identification and evaluation of 70 WRD and 54 LWD. The results obtained demonstrate the capability of the proposed approach

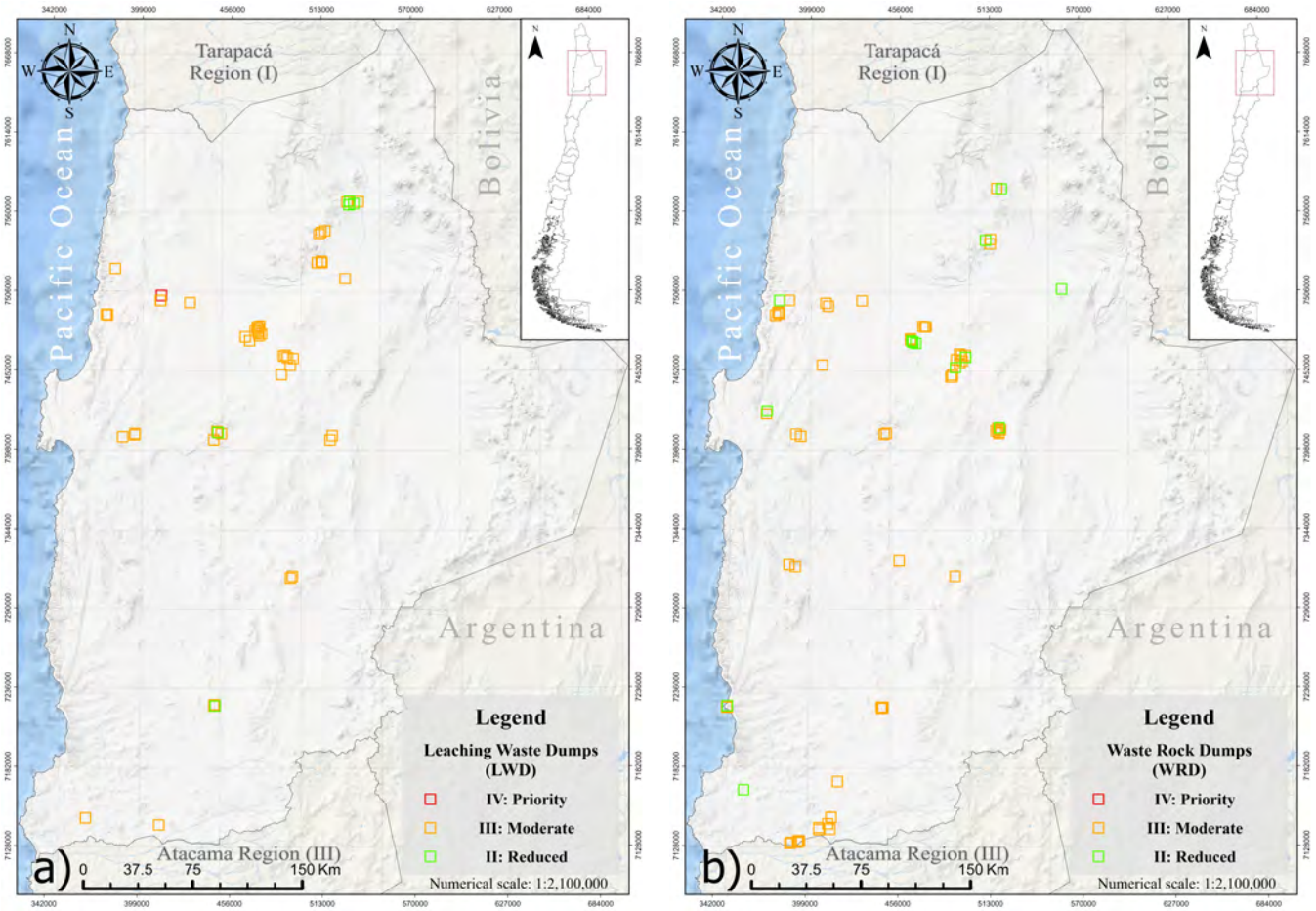

FIGURE 10: Georeferencing of LWDs and WRDs detected and evaluated in the Antofagasta region. IPL: a) LWD, b) WRD.

to prioritize deposits according to their potential risk, thereby facilitating the supervision and oversight work of SERNAGEOMIN. The successful application in this region suggests that the methodology can be extended to other mining areas and adapted to different types of facilities, including tailings storage facilities.

VIII. ACKNOWLEDGEMENTS

The authors gratefully acknowledge the valuable contribution of SERNAGEOMIN in validating the information used and providing feedback for the evaluation methodology proposed in this work. We also extend our sincere thanks to undergraduate students from the School of Electrical Engineering at Pontificia Universidad Católica de Valparaíso—Rodrigo Pereira, Gonzalo Caballero, and Felipe Aravena—and to geographer Emilio Bustos, who contributed to the downloading and labeling of the database.

IX. FUNDING

This research was funded and supported by the Vice-Rectorate for Research, Creation, and Innovation (VINCI) at Pontificia Universidad Católica de Valparaíso (Chile), through the Associative Research Project DI (under grant: 039.301/2024), Centennial Project 2024 (under grant: 039.310/2024), FONDECYT under Grant 1240573, and ANID Doctorado Nacional 2023-21232328.

REFERENCES

[1] COCHILCO, "Monitoreo del estado de los relaves mineros en chile."
[2] M. Silva, G. Hermosilla, G. Villavicencio, and P. Breul, "Automated detection and analysis of massive mining waste deposits using sentinel-2 satellite imagery and artificial intelligence," vol. 15, no. 20.
[3] G. Earth, "El soldado, nogales, chile." Version Number: 7.3.6.9796 Published: Accessed: November 18, 2024.
[4] G. Earth, "BioCobre, copiapó, chile." Version Number: 7.3.6.9796 Published: Accessed: November 18, 2024.
[5] Ministerio de Minería, Chile, "Decreto n° 41: Aprueba el reglamento de la ley de cierre de faenas e instalaciones mineras [in spanish]."
[6] Ministerio Secretaría General de la Presidencia, Chile, "Ley 19.300: Aprueba ley sobre bases generales del medio ambiente [in spanish]."
[7] British Columbia Ministry of Energy and Mines, "Investigation and design manual interim guidelines, mine rock and overburden piles." Place: British Columbia, Canada.
[8] M. Hawley and J. Cunning, *Guidelines for Mine Waste Dump and Stockpile Design*. CSIRO Press/Balkema.
[9] SERNAGEOMIN, "Guía metodológica para evaluación de la estabilidad física de instalaciones mineras remanentes."
[10] Ministerio de Minería, Chile, "Ley n° 20.551: Regula el cierre de faenas e instalaciones mineras [in spanish]."

[11] A. Fourie, G. Villavicencio, J. Palma, P. Valenzuela, and P. Breul, "Evaluation of the physical stability of leaching waste deposits for the closure stage," in *Proceedings of the 20th International Conference on Soil Mechanics and Geotechnical Engineering (ICSMGE 2022)*.
[12] J. C. Quezada and G. Villavicencio, "Characterisation of the internal friction angle of waste rock material from large triaxial tests using the contact dynamics method," vol. 0, no. 0, pp. 1–20. Publisher: Taylor & Francis _eprint: https://doi.org/10.1080/17480930.2024.2367977.
[13] E. Ferreira, M. Brito, R. Balaniuk, M. S. Alvim, and J. A. d. Santos, "Brazildam: A benchmark dataset for tailings dam detection," in *2020 IEEE Latin American GRSS & ISPRS Remote Sensing Conference (LAGIRS)*, pp. 339–344.
[14] G. V. Arancibia, O. P. Bustamante, G. H. Vigneau, H. Allende-Cid, G. S. Fuentelaba, and V. A. Nieto, "Estimation of moisture content in thickened tailings dams: Machine learning techniques applied to remote sensing images," vol. 9, pp. 16988–16998.
[15] A. Pepe and F. Calò, "A review of interferometric synthetic aperture RADAR (InSAR) multi-track approaches for the retrieval of earth's surface displacements," vol. 7, no. 12.
[16] X. Wu, X. Qi, B. Peng, and J. Wang, "Optimized landslide susceptibility mapping and modelling using the SBAS-InSAR coupling model," vol. 16, no. 16.
[17] D. Yan, G. Li, X. Li, H. Zhang, H. Lei, K. Lu, M. Cheng, and F. Zhu, "An improved faster r-CNN method to detect tailings ponds from high-resolution remote sensing images," vol. 13, no. 11.
[18] F. Pacheco, G. Hermosilla, O. Piña, G. Villavicencio, H. Allende-Cid, J. Palma, P. Valenzuela, J. García, A. Carpanetti, V. Minatogawa, G. Suazo, A. León, R. López, and G. Novoa, "Generation of synthetic data for the analysis of the physical stability of tailing dams through artificial intelligence," vol. 10, no. 23.
[19] I. Atif, F. T. Cawood, and M. A. Mahboob, "Modelling and analysis of the brumadinho tailings disaster using advanced geospatial analytics," vol. 120, no. 7, pp. 405–414.
[20] S. K. Sarker, N. Haque, W. Bruckard, M. Bhuiyan, and B. K. Pramanik, "Development of a geospatial database of tailing storage facilities in australia using satellite images," vol. 303, p. 135139.
[21] S.-I. Balaban, K. A. Hudson-Edwards, and J. R. Miller, "A GIS-based method for evaluating sediment storage and transport in large mining-affected river systems," vol. 74, no. 6, pp. 4685–4698.
[22] R. Verdugo, "Seismic site classification," vol. 124, pp. 317–329.
[23] "Mapa geológico de chile," Publisher: SERNAGEOMIN.
[24] D. C. Heath, D. J. Wald, C. B. Worden, E. M. Thompson, and G. M. Smoczyk, "A global hybrid VS30 map with a topographic slope–based default and regional map insets," vol. 36, no. 3, pp. 1570–1584. _eprint: https://doi.org/10.1177/8755293020911137.
[25] IDE, "DEM alos palsar región de antofagasta."
[26] Instituto Nacional de Normalización (INN), *Earthquake Resistant Design of Buildings, NCh 433.Of 96_Mod 2012 [in Spanish]*. Instituto Nacional de Normalización.
[27] V. Maldonado, M. Contreras, and D. Melnick, "A comprehensive database of active and potentially-active continental faults in chile at 1:25,000 scale," vol. 8, no. 1, p. 20.
[28] Sistema Nacional de Información de Aguas Terrestres (SNIAT), "Sistema nacional de información de aguas terrestres."
[29] M. Tkachenko, M. Malyuk, A. Holmanyuk, and N. Liubimov, "Label studio: Data labeling software."
[30] G. Jocher, J. Qiu, and A. Chaurasia, "Ultralytics YOLO." original-date: 2022-09-11T16:39:45Z.
[31] K. He, X. Zhang, S. Ren, and J. Sun, "Deep residual learning for image recognition." _eprint: 1512.03385.

GABRIEL HERMOSILLA VIGNEAU was born in Chillan, Chile, in 1982. He received the degree in electronic engineering from the University of La Frontera, Temuco, Chile, in 2007, and the Ph.D. degree in electric engineering from the University of Chile, Santiago, Chile, in 2012. Currently, he is an Associate Professor with the School of Electrical Engineering, Pontificia Universidad Católica de Valparaiso (PUCV), Valparaiso, Chile. His main areas of research interest are thermal face recognition, pattern recognition, computer vision, and deep learning.

GABRIEL VILLAVICENCIO ARANCIBIA was born in Valparaíso, Chile in 1977. He received the Ph.D. degree in civil engineering from Ecole Doctorale des Sciences pour l'Ingénieur. Université Blaise Pascal, Clermont II, France in 2009. From 2004 to 2009, he was a temporary teaching and research associates with the civil engineering department, Polytech Clermont-Ferrand, France. Since 2010 to date, he has been an assistant professor with the Construction and Transportation Engineering of the Pontificia Universidad Católica de Valparaíso, and geotechnical engineer with the LEPUCV laboratory. His research interests include geotechnical engineering applications for tailings storage facilities (TSF), wasted rocks dumps and leaching waste dumps. In addition, in topics such as physical stability TSF, evaluation of liquefaction potential, slope stability and geotechnical modeling of urban sites. He is an active member of the Chilean Geotechnical Society.

GIOVANNI COCCA GUARDIA (Member, IEEE) was born in Calama, Chile. He received his B.Sc. degree in Engineering Sciences and his Civil Electrical Engineering degree from the Pontificia Universidad Católica de Valparaíso, where he is currently pursuing an M.Sc. degree. His research interests include Graph Neural Networks, Electrical Power System, Generative AI and Efficient Learning AI.

VICENTE APRIGLIANO Professor at the School of Construction and Transportation Engineering at PUCV, Valparaíso, Chile. He completed a post-doctoral fellowship at the Center for Sustainable Urban Development (PUC-Chile) and holds a PhD in Human Geography from Universität Tübingen, Germany. With a Master's in Transportation Engineering (COPPE/UFRJ) and a Bachelor's in Geography (UFRJ), his research focuses on transport geography, economic geography, urban geography, and urban mobility planning.

MANUEL SILVA VEGA (Member, IEEE) was born in Valparaíso, Chile, in 1990. He received his BS in Electronics Engineering in 2022 and his MSc in Electrical Engineering in 2023 from the School of Electrical Engineering at the Pontificia Universidad Católica de Valparaiso.

He is currently pursuing a Ph.D. in Electrical Engineering in the Robotics and Vision Lab at the same university, where his research focuses on computer vision, remote sensing, machine learning, and robotics.

JUAN CARLOS QUEZADA was born in Valparaíso, Chile, in 1982. He completed his undergraduate studies at the Pontificia Universidad Católica de Valparaíso, earning a degree in Construction Engineering in 2008. In 2009, he obtained a Master's degree from the University Blaise Pascal (Clermont II) in France. From 2009 to 2012, he pursued a doctoral degree through a collaborative program between the University Montpellier II in France and the French National Railway Company (SNCF), culminating in a Ph.D. in Mechanics and Civil Engineering. Following his doctoral studies, Dr. Quezada worked as an engineer in the Innovation and Research Department of SNCF in Paris, France, until 2014. He then joined the LTDS Laboratory at École Centrale de Lyon, France, as a postdoctoral researcher, where he focused on the numerical modeling of dry-stone retaining walls. In 2015, he was appointed Associate Professor in the Civil Engineering Department at INSA Strasbourg, France, a position he continues to hold. His teaching portfolio encompasses topics in structural engineering, geotechnics, and numerical methods. Dr. Quezada is an active researcher affiliated with the ICube Laboratory, where his work centers on numerical modeling using Discrete Element Method (DEM) and Finite Element Method (FEM) in geomechanics, with applications to geomaterials.

PIERRE BREUL was born in France, in 1972. He received the degree in civil engineering from the University Blaise Pascal, Clermont-Ferrand, France, in 1995, and the Ph.D. degree in civil engineering from the University Blaise Pascal, Clermont-Ferrand, France, in 1999. After having been engineer for 5 years in a geotechnical engineering company, he is currently Professor at the National Polytechnic Institute of Clermont Auvergne University and head of the engineering school Polytech Clermont. His research interests include geotechnics, soils and granular materials mechanics, images and data analysis for soils recognition and identification, infrastructure diagnosis and risk analysis.

VINICIUS MINATOGAWA was born in Americana, São Paulo, Brazil, in 1990. He received the Ph.D. degree in Mechanical Engineering and the M.Sc. degree from the University of Campinas, Brazil. Since 2021 to date, he has been an Associate Professor with the Construction and Transportation Engineering School of the Pontificia Universidad Católica de Valparaíso. His research interests include digital transformation projects, aiming to integrate emerging technologies, data-driven decision-making, and organizational innovation in engineering and related sectors. In addition, he is a Project Management Professional (PMP®) certified by the Project Management Institute (PMP®Number: 3778535), with a particular focus on agile projects. His work has been featured in high-impact journals such as Automation in Construction, the Review of Managerial Science, and the Journal of Manufacturing Technology Management.

JAIME WILSON MORALES SAAVEDRA , born in the Maria Elena saltpeter office in 1973. Professional trained in teaching and research, with communication and leadership skills. Experience in teaching in the area of Thermodynamics and Unit Operations, applying evaluation concepts through competencies and strategies of new evaluation alternatives. Development of research in the study of Thermodynamic, Volumetric and Transport Properties applying Electrochemistry, Thermodynamic Modeling in Systems Containing Electrolytes and Electrochemistry of Lithium Batteries, chemical stability of tailings and slag valorization based on circular economy.

APPENDIX A GIS CARTOGRAPHY

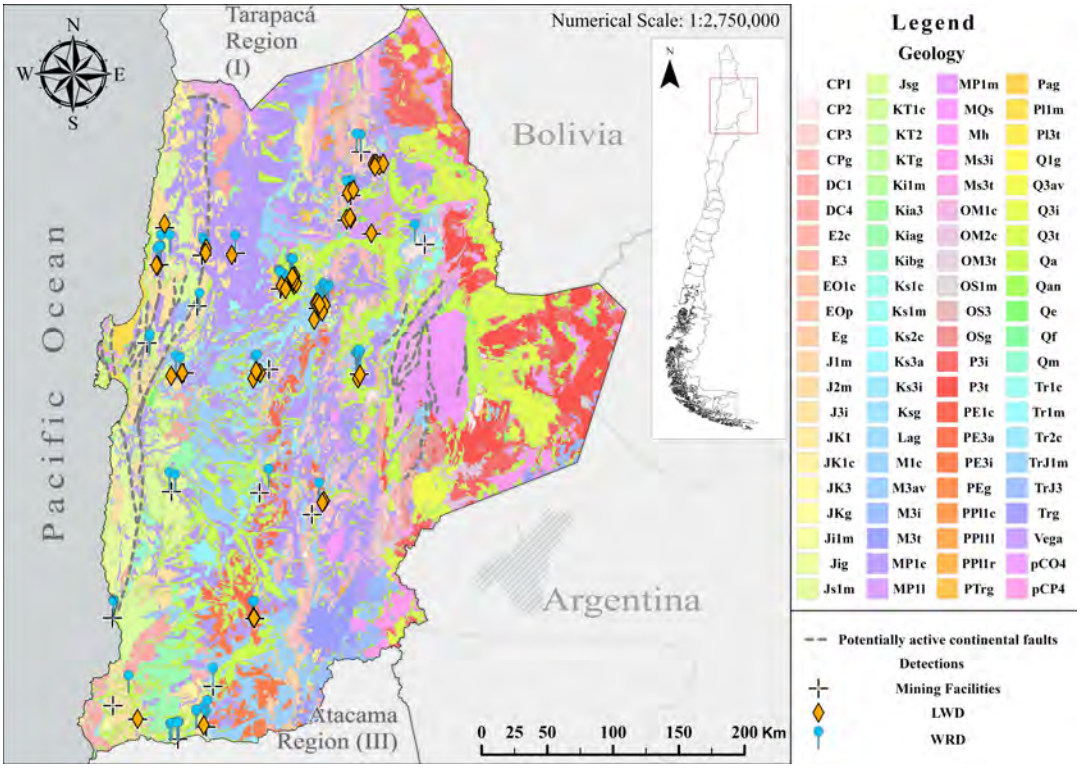

FIGURE A.1: Geological map of Chile, scale 1:1,000,000. Antofagasta region, Chile. SERNAGEOMIN (2002).

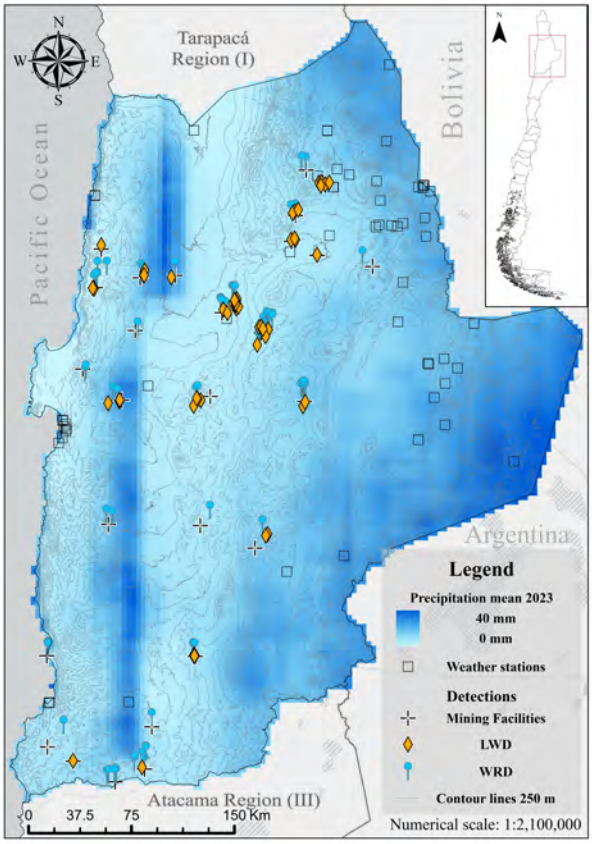

FIGURE A.2: Precipitation mean 2023. Antofagasta region, Chile. SNIAT (2024)

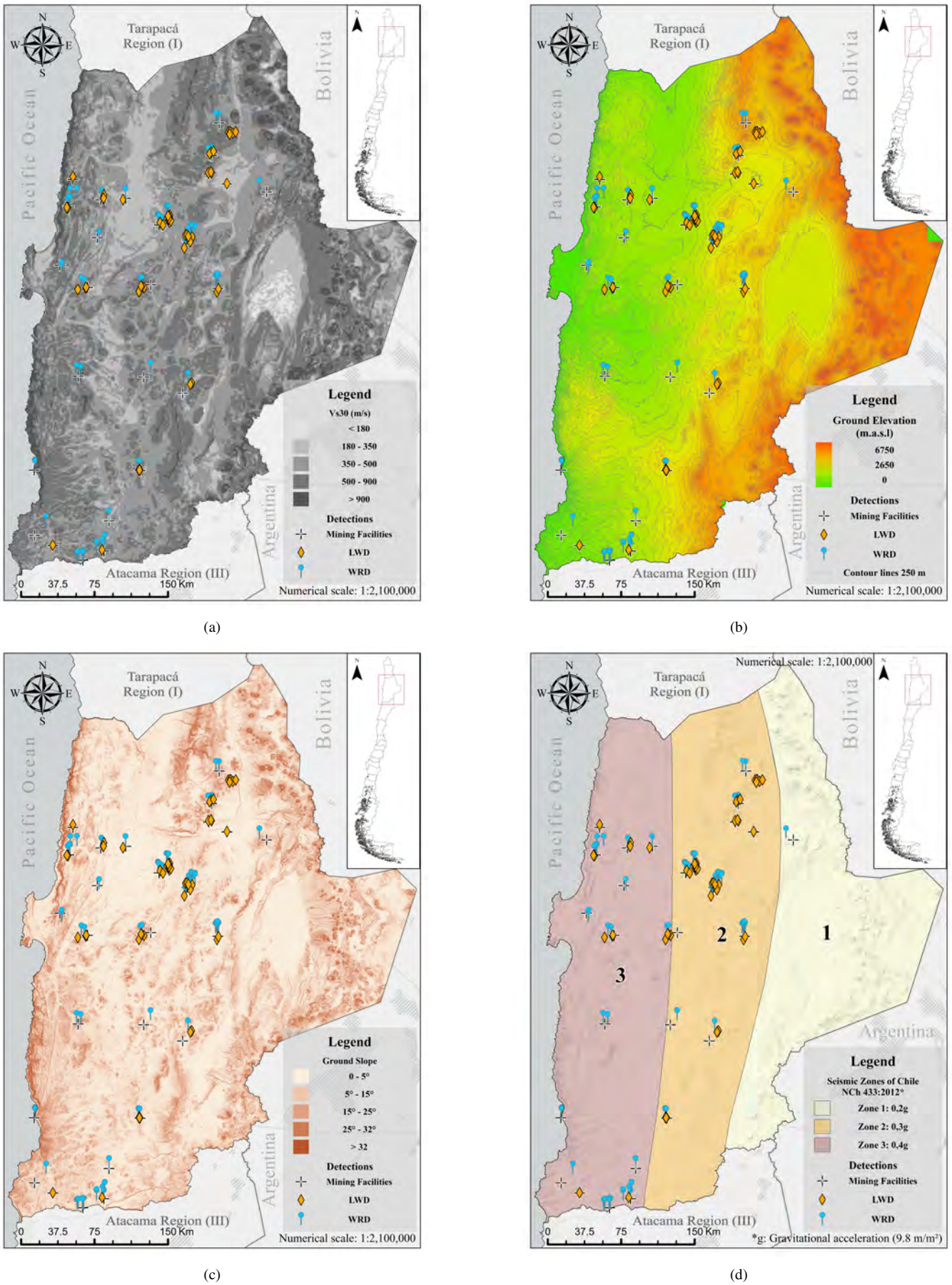

(a) (b)

(c) (d)

FIGURE A.3: Antofagasta region, Chile. a) Global Vs_{30} Mosaic Map Viewer. Heath et al. (2020). b) Digital elevation models. Chile. IDE (2016). c) Slope geoprocessing of digital elevation models. Antofagasta region, Chile. IDE (2016). d) Seismic zones of Chile. Antofagasta region. INN (2012).